

Structural and Catalytic Properties of Silica-Coated Alumina

Satoshi Sato,* Ryoji Takahashi, Toshiaki Sodesawa, Daiji Shin,
Naoki Ichikawa, and Katsuyuki Ogura

Department of Applied Chemistry, Faculty of Engineering, Chiba University, 1-33 Yayoi, Inage-ku, Chiba 263-8522

Received July 12, 2005; E-mail: satoshi@faculty.chiba-u.jp

SiO₂-coated Al₂O₃ powders were prepared by depositing hydrolyzed tetraethoxysilane (TEOS) on Al(OH)₃ and γ -Al₂O₃ at 40 °C. In the preparation using Al(OH)₃ with a specific surface area (SA) of ca. 40 m² g⁻¹ as a support, loading of silica deposited on the Al(OH)₃ was saturated at 80 mg g_{alumina}⁻¹. Ammonium nitrate, a catalyst for the hydrolysis of TEOS, increased silica loading linearly with increasing the amount of TEOS charged, while the silica aggregated on the Al(OH)₃. At temperatures of >300 °C, the core Al(OH)₃ coated with aggregated silica was fragmented into a mixture of small particles of pure alumina and silica–alumina diminishing small particles with a large SA of >400 m² g⁻¹. The small surface area of the support Al(OH)₃ is ineffective in generating active acid sites. In the deposition of silica on γ -Al₂O₃ with a SA of 450 m² g⁻¹, however, silica loading increased with increasing the amount of TEOS charged at 40 °C without using ammonium nitrate. Silicate species with thinner layer structures uniformly covered the γ -Al₂O₃ surface. The SiO₂-covered γ -Al₂O₃ showed higher catalytic activity than the SiO₂-Al₂O₃ prepared from Al(OH)₃ did.

We have recently prepared various metal oxides coated with silica by liquid-phase deposition using tetraethoxysilane (TEOS).^{1,2} The silica-coated metal oxides of MgO, Fe₂O₃, NiO, Y₂O₃, ZrO₂, SnO₂, and Dy₂O₃ have high specific surface areas (SA) of >200 m² g⁻¹ even after heating at 500 °C.¹ The silica species deposited on the surface of the primary hydroxide particles prohibit the core oxide particles from agglomerating during calcination, although the primary particles of the pure hydroxides readily aggregate into large oxide particles.^{1,2} We have also reported another silica deposition: silica dissolved in an aqueous basic solution deposits on precipitates of ZrO(OH)₂ and Ni(OH)₂ under hydrothermal conditions at 100 °C.^{3,4} In the liquid-phase silica deposition, TEOS treatment is more efficient for silica deposition than hydrothermal treatment employing the dissolution–deposition of silica.²

In vapor-phase deposition processes,^{5–7} we have prepared SiO₂-Al₂O₃ by depositing silica on alumina supports using TEOS vapor. Vapor-phase deposition of silica has been studied on other supports such as ZrO₂ and TiO₂.^{8,9} Support materials limit the SA of the resulting composite catalysts in the vapor-phase process: the SA of the alumina used was at most 200 m² g⁻¹.^{5–7} In contrast, the liquid-phase process has an advantage in depositing silica, because the deposition proceeds under mild conditions utilizing the high surface area of the oxide and hydroxide precursors.

In our preliminary tests, we examined the treatment of several metal hydroxides in a basic solution with silica glass chips under hydrothermal conditions.¹ It was found that no silica deposition occurred upon the hydroxides of Al(III) and Ti(IV) at pH 10. Since the isoelectric point of aluminum hydroxide is close to the pH of the deposition conditions,¹⁰ we are afraid that the bonds of Si–O–Al and Si–O–Ti are unstable near the isoelectric points. Then, we expect that the silica deposition using TEOS would be promising for the preparation of fine

particles of SiO₂-coated aluminum oxide. In the preparation of an alumina support, Al(OH)₃ precipitate is transformed to alumina at around 300 °C.¹¹ The transformation of Al(OH)₃ into alumina increases the SA, where the SA of the Al(OH)₃ precipitate, derived from neutralization of aluminum(III) nitrate solution and dried at 100 °C, is only 35 m² g⁻¹.¹²

In this paper, we examine the deposition behavior of silica on either an Al(OH)₃ precipitate or γ -Al₂O₃ powder using TEOS, where Al(OH)₃ precipitated freshly and alumina obtained by calcining the Al(OH)₃ precipitate at 300 °C are used as the support. We clarify the effect of the properties of the support material for the liquid-phase silica deposition. We also discuss the structure of the resulting SiO₂-coated Al₂O₃ after calcination at 500 °C in connection with the catalytic behaviors for the cracking of cumene.

Experimental

Samples. All reagents were supplied by Wako Pure Chemical Industry (Japan). A precipitate of Al(OH)₃ was obtained by adding 10 wt % of an Al(NO₃)₃ solution (51 g) into 5.0 mol dm⁻³ of an ammonia solution (194 g). After filtration and removal of ammonia by washing with distilled water, the fresh precipitate containing ca. 8 g of water and 19.6 mmol-Al, which corresponds to 1 g of the resulting Al₂O₃, was used for the following silica deposition. Figure 1 depicts the outline of the preparation procedure for the silica deposition with three different types.

As-prepared hydroxide precipitate was placed in a glass vessel with ethanol (30 g) and TEOS (0.348–2.08 g; ex. 0.693 g of TEOS corresponds to 200 mg of silica). The hydroxide precipitate suspended in the solution was stirred at 40 °C for a prescribed period. The precipitate collected by filtration was dried at 50 °C for 12 h, followed by 110 °C for 12 h to obtain a SiO₂-Al(OH)₃ sample. Then, it was calcined in air at 500 °C for 3 h at a heating rate of 1 K min⁻¹ to obtain a SiO₂-Al₂O₃ sample (series A₀). In Fig. 2, silica loading was calculated from the difference between the

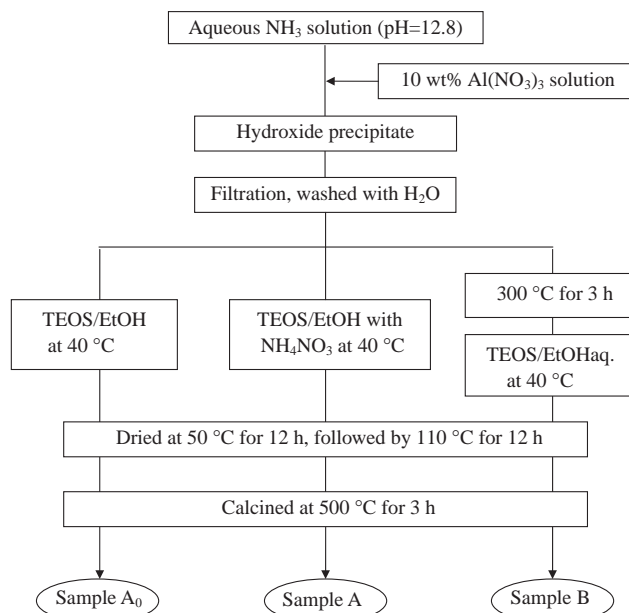


Fig. 1. Procedure for the preparation of SiO₂-Al₂O₃ samples.

charged TEOS and residual TEOS, which was determined by the weight of silica precipitate recovered by evaporation of the filtrate solution after hydrolysis of the residual TEOS by an aqueous NaOH solution.

Another silica deposition over the hydroxide precipitate was examined by adding 0.13 g of ammonium nitrate as a catalyst for the hydrolysis of TEOS in the TEOS/ethanol solution. The suspended solution was stirred at 40 °C for a prescribed period. Then, the sample was collected by filtration, dried at 110 °C, and calcined at 500 °C in the same manner as the previous sample, A₀. The resulting SiO₂-Al₂O₃ sample is called series A. For example, the sample name A-400 indicates a series-A sample with silica loading of 400 mg g_{alumina}⁻¹.

Another series of SiO₂-Al₂O₃ was prepared using γ -Al₂O₃ as a support for the silica deposition (series B). The γ -Al₂O₃ support with the specific surface area of 450 m² g⁻¹ was obtained by heating the as-prepared hydroxide precipitate at 300 °C for 3 h. The Al₂O₃ sample was put in a glass vessel with ethanol (30 g), water (8.0 g), and TEOS (0.348–2.08 g). The suspended solution was stirred at 40 °C for a prescribed period, until a white precipitate caused by abrupt hydrolysis and polymerization of TEOS was not observed when aqueous NaOH solution was added to the extracted supernatant solution. Then, the sample was collected by filtration, dried at 110 °C, and calcined at 500 °C in the same manner as sample A₀ mentioned above.

A commercial silica-alumina, N-631L, purchased from Nikki Chemicals (Japan) was used as a reference catalyst. The silica-alumina has an alumina content of 13 wt % and SA of 405 m² g⁻¹.

Characterization. The SA of the samples was determined by the BET method using the N₂ adsorption isotherm measured with a conventional volumetric gas adsorption apparatus at -196 °C. Prior to the N₂ adsorption, samples were heated in a vacuum at 300 °C for 1 h, while samples calcined at temperatures lower than 300 °C were heated at 100 °C. XRD profiles of samples were recorded on a M18XHF (Mac Science, Japan).

Magic angle spinning (MAS) NMR spectra were recorded on a DPX-300 multinuclear spectrometer (Bruker, Germany). ²⁷Al MAS NMR was measured at 78.23 MHz at MAS speed of

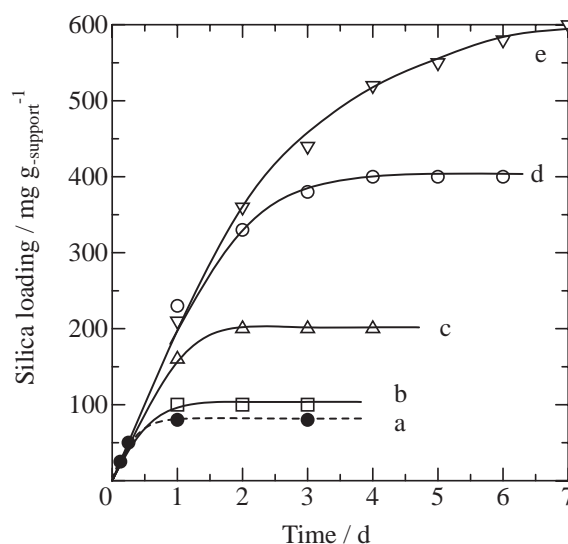


Fig. 2. Deposition behavior of SiO₂ from TEOS on Al(OH)₃ and Al₂O₃. a, sample A₀ using 0.693 g of TEOS (corresponding to 200 mg of SiO₂); b, sample A, 0.347 g (100 mg); c, sample A, 0.693 g (200 mg); d, sample A, 1.39 g (400 mg); e, sample A, 2.08 g (600 mg).

5.80 kHz; 8192 free induction decays (FID) were accumulated with radio-frequency pulses of 0.3 μ s, which correspond to 5.4° tip, and repetition delay times of 0.5 s. The ²⁷Al chemical shifts (in ppm) are referenced to a 1.0 mol dm⁻³ Al(NO₃)₃ solution used as an external standard. ²⁹Si MAS NMR spectra were obtained with high power ¹H decoupling at 59.64 MHz at a MAS speed of 4.00 kHz; 1024–2048 FID signals were accumulated with radio-frequency pulses of 1.6 μ s, which correspond to 30° tip, and a repetition delay time of 60 s. The ²⁹Si chemical shifts are referenced to tetramethylsilane (TMS) using sodium 4,4-dimethyl-4-silapentanesulfonate (DSS, 1.534 ppm) as an external standard.

A temperature-programmed desorption (TPD) of adsorbed benzaldehyde (BA) was done in N₂ flow: details of the procedure have been reported elsewhere.² Prior to adsorption of BA, a sample (20 mg) fixed in a quartz tube was heated at 500 °C for 1 h. After the sample had been cooled to 250 °C, five pulses of BA, with each pulse being 10 mm³, were injected in an N₂ flow of 50 cm³ min⁻¹. BA desorbed from the sample was monitored on a flame-ionization detector from 250 to 800 °C at a heating rate of 10 K min⁻¹. Since BA is adsorbed not on silica but on alumina,^{13,14} we can calculate the surface density of the adsorbed BA, which means the exposure of Al(III) oxide on the surface.

TPD of adsorbed NH₃ was measured by monitoring the electric conductivity of a diluted sulfuric acid solution, into which NH₃ desorbed from the sample was bubbled with N₂ carrier gas. Details of the procedure have been reported elsewhere.^{15,16} After the sample had been evacuated at 500 °C under a reduced pressure of 1.3 Pa, NH₃ vapor was introduced at 13.3 kPa and 100 °C, followed by evacuation at 100 °C for 1 h. The TPD was performed at a heating rate of 10 K min⁻¹ from 100 to 800 °C in an N₂ flow of 54 cm³ min⁻¹ after no NH₃ desorbed at 100 °C was detected.

Catalytic tests for the cumene-cracking reaction were performed in a pulse reactor using a sample of 10 mg in a H₂ flow at temperatures of 200–500 °C. The details have been described elsewhere.¹⁷ No significant difference was observed in the catalytic activities of silica-alumina under H₂- and He-flow conditions.

Results

Deposition of Silica on $\text{Al}(\text{OH})_3$ and Al_2O_3 . Prior to silica deposition, we examined the physical properties of supports of $\text{Al}(\text{OH})_3$ and Al_2O_3 with different heating temperatures. Table 1 summarizes the SA and average particle size of the supports and their crystal structure. The SA of aluminum hydroxide is as small as $40 \text{ m}^2 \text{ g}^{-1}$. With increasing the heating temperature, the SA abruptly increases to $450 \text{ m}^2 \text{ g}^{-1}$ at 300°C and decreases gradually above 300°C . At ca. 300°C , $\text{Al}(\text{OH})_3$ was transformed into $\gamma\text{-Al}_2\text{O}_3$. The transformation accompanies with the decomposition of a large $\text{Al}(\text{OH})_3$ particle into small pieces of $\gamma\text{-Al}_2\text{O}_3$ particles. Then, we prepare silica-coated alumina samples using both a fresh $\text{Al}(\text{OH})_3$ precipitate (series A₀ and A) and $\gamma\text{-Al}_2\text{O}_3$ heated at 300°C (series B) in order to clarify the effect of the properties of the support material for silica deposition.

Figure 2 shows the changes in silica loading with time of immersion for preparation at different TEOS concentrations.

Table 1. Structure of $\text{Al}(\text{OH})_3$ with Different Heating Temperature

Temperature / $^\circ\text{C}$	Structure ^{a)}	SA ^{b)} / $\text{m}^2 \text{ g}^{-1}$	Particle size ^{c)} /nm
as-prepared ^{d)}	$\text{Al}(\text{OH})_3$ + amorphous	—	—
110	$\text{Al}(\text{OH})_3$	42	66
200	$\text{Al}(\text{OH})_3$	12	200
300	$\gamma\text{-Al}_2\text{O}_3$	450	3.9
400	$\gamma\text{-Al}_2\text{O}_3$	424	4.2
500	$\gamma\text{-Al}_2\text{O}_3$	300	5.9

a) Determined by XRD. b) Specific surface area. c) Average particle diameter, d , calculated from the equation, $d = 6/SA/\rho$, where ρ is the density of either bayerite, 2.5 g cm^{-3} , or γ -alumina, 3.4 g cm^{-3} . d) Wet precipitate.

In the preparation of samples A₀, silica loading was saturated at only $80 \text{ mg g}_{\text{alumina}}^{-1}$, even with the use of excess TEOS. In the preparation of series-A samples using ammonium nitrate as a catalyst for the hydrolysis of TEOS, silica loading increased with immersion time, and all the TEOS charged in the vessel deposited on the $\text{Al}(\text{OH})_3$ for a sufficient period. The silica loading well agrees with the amount of TEOS charged. In the preparation of series-B $\text{SiO}_2\text{-Al}_2\text{O}_3$, silica loading also agrees with the amount of TEOS charged without using ammonium nitrate as a hydrolysis catalyst.

Table 2 lists the SAs of the $\text{SiO}_2\text{-Al}_2\text{O}_3$ samples. In the absence of TEOS, the original alumina prepared by heating the fresh $\text{Al}(\text{OH})_3$ precipitate at 500°C has a large SA ($300 \text{ m}^2 \text{ g}^{-1}$). In samples A₀ and A, SAs are as high as $350\text{--}400 \text{ m}^2 \text{ g}^{-1}$, while those of the as-dried samples are as low as $30\text{--}40 \text{ m}^2 \text{ g}^{-1}$. The core $\text{Al}(\text{OH})_3$ particles are decomposed into alumina at temperatures between 200 and 300°C , as shown in Table 1. In the series-B samples, however, SAs are constant at ca. $300 \text{ m}^2 \text{ g}^{-1}$, which is the same as that of the original support alumina calcined at 500°C .

Structure of Silica-Coated Alumina. Figure 3 depicts the XRD profiles of several samples dried at 110°C and heated at 500°C . In $\text{Al}(\text{OH})_3$ and A-400 dried at 110°C (Figs. 3a and 3b), the diffraction peaks at $2\theta = 19.0, 20.8, 28.3, 40.8, 53.6$, and 63.9 degrees are assigned as planes of bayerite, $\text{Al}(\text{OH})_3$. In the samples of $\gamma\text{-Al}_2\text{O}_3$ and A-400 calcined at 500°C (Figs. 3c and 3d), the diffraction peaks at $2\theta = 20.0, 37.9, 39.6, 46.0, 61.0$, and 67.0 degrees are assigned as planes of γ -alumina. The crystal structures of the samples heated at 110 and 500°C are $\text{Al}(\text{OH})_3$ and $\gamma\text{-Al}_2\text{O}_3$, respectively. They are independent of silica deposition.

Figure 4 illustrates ^{27}Al MAS NMR spectra of samples with different heat treatment. In the samples of $\text{Al}(\text{OH})_3$ and A-400 dried at 110°C (Figs. 4a and 4b), the peak at 0 ppm shows 6-coordinate Al. In the samples of $\gamma\text{-Al}_2\text{O}_3$ and A-400 calcined

Table 2. Physical and Catalytic Properties of SiO_2 -Coated Al_2O_3 ^{a)}

Catalyst	Silica loading / $\text{mg g}_{\text{alumina}}^{-1}$	SA ^{b)} / $\text{m}^2 \text{ g}^{-1}$	Silica density ^{c)} / nm^{-2}	Thickness of silica ^{d)} /nm	Conversion/ $\%$ ^{e)}		
					400°C	450°C	500°C
Al_2O_3	0	300 (300)	0	0	0	0	0
A ₀ -80	80	400 (432)	1.9	0.08	0.1	1.2	3.2
A-100	100	365 (402)	2.5	0.11	1.5	3.3	7.2
A-200	200	345 (414)	4.8	0.22	10.5	19.1	33.2
A-300	300	350 (455)	6.6	0.30	12.7	26.7	42.6
A-400	400	345 (483)	8.3	0.38	20.6	38.2	57.6
A-500	500	370 (555)	9.0	0.41	24.6	41.2	59.6
A-600	600	400 (640)	9.4	0.43	12.1	20.6	33.1
B-100	100	310 (341)	2.9	0.13	1.8	4.1	9.3
B-200	200	295 (354)	5.7	0.26	13.0	23.3	37.2
B-400	400	310 (434)	9.2	0.42	48.3	68.9	84.4
B-600	600	305 (488)	12.3	0.56	43.1	63.0	72.1

a) Calcined at 500°C for 3 h. b) Specific surface area, a number in the parentheses expresses the specific surface area, SA' , based on the weight of core alumina. c) Surface silica density (d) is calculated from the equation, $d = 6.02 \times 10^{23} [\text{mol}^{-1}] \times (\text{silica loading } [\text{mg g}_{\text{support}}^{-1}]) / (1000 + \text{silica loading}) / 60 [\text{g mol}^{-1}] / (\text{specific surface area } [\text{m}^2 \text{ g}^{-1}])$. d) Average thickness (t) of SiO_2 layer deposited on alumina is calculated using the following equation, $t = (\text{silica loading } [\text{mg g}_{\text{support}}^{-1}]) / (1000 + \text{silica loading}) / 2.2 [\text{g cm}^{-3}] / (\text{specific surface area } [\text{m}^2 \text{ g}^{-1}])$, where the density of amorphous silica is assumed to be 2.2 g cm^{-3} . e) Cumene cracking was carried out at the prescribed temperatures.

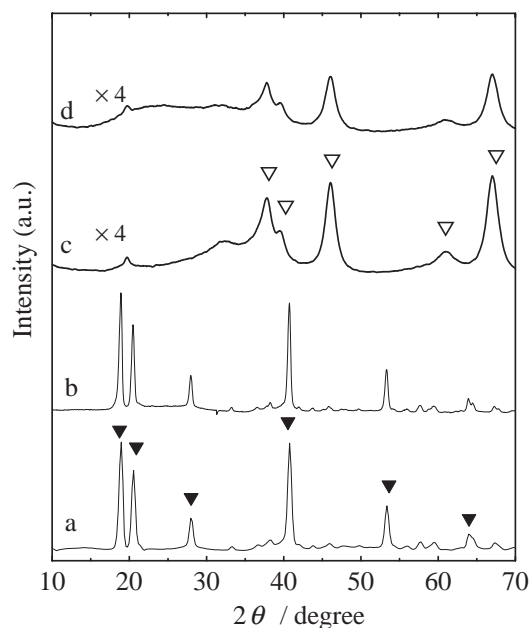


Fig. 3. XRD profiles of SiO₂-Al₂O₃ samples. a, Al(OH)₃ dried at 110 °C; b, A-400 dried at 110 °C; c, Al₂O₃ heated at 500 °C; d, A-400 heated at 500 °C. ▼: Al(OH)₃, ▽: γ-Al₂O₃.

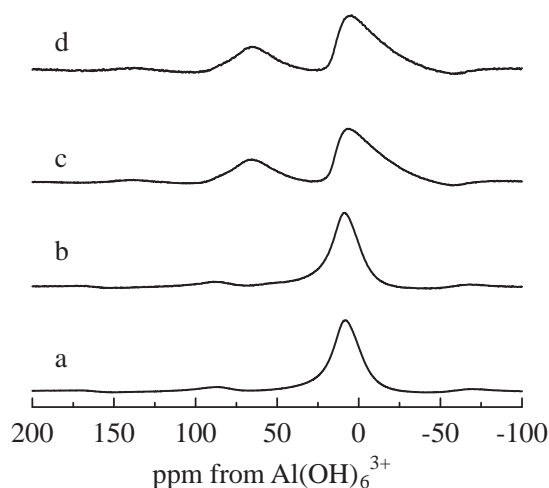


Fig. 4. ²⁷Al MAS NMR spectra of SiO₂-Al₂O₃. Symbols are the same as those in Fig. 3.

at 500 °C (Figs. 4c and 4d), the peaks at 0 and 65 ppm indicate 6-coordinate and 4-coordinate Al, respectively. There were no significant differences in the ²⁷Al NMR spectra between the samples with and without silica deposition. The NMR results are consistent with the XRD results depicted in Fig. 3.

Figure 5 depicts ²⁹Si MAS NMR spectra of SiO₂-Al₂O₃ calcined at 500 °C. In both series A and B, the major ²⁹Si resonance peak observed at -78 ppm shifted to -110 ppm with increasing silica loading. In series A, however, a broad peak is observed at around -110 ppm, even at the low silica loading of 100 mg g_{alumina}⁻¹. In sample A₀-80, the major peak is observed at ca. -78 ppm, and the spectrum is similar to that of B-100.

Figure 6 shows a change in the density of adsorption sites of

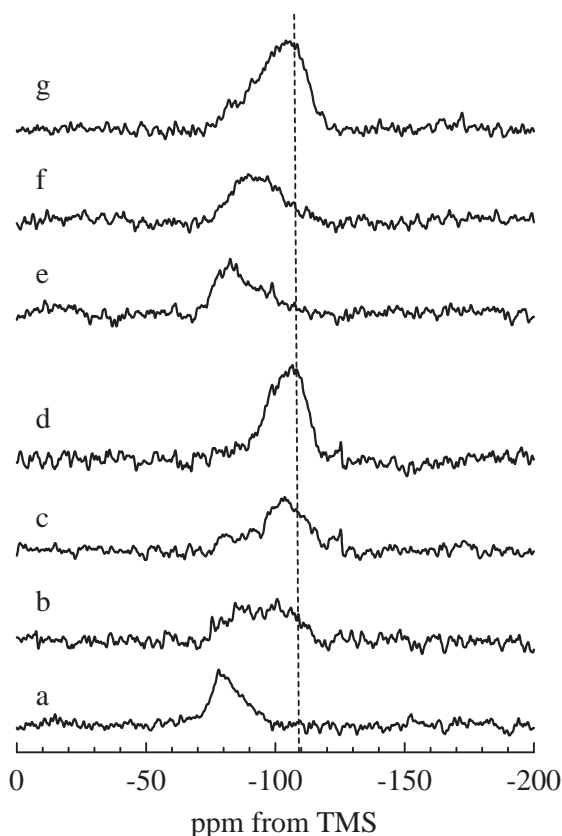


Fig. 5. ²⁹Si MAS NMR spectra of SiO₂-Al₂O₃ heated at 500 °C. a, sample A₀-80; b, A-100; c, A-200; d, A-400; e, B-100; f, B-200; g, B-400.

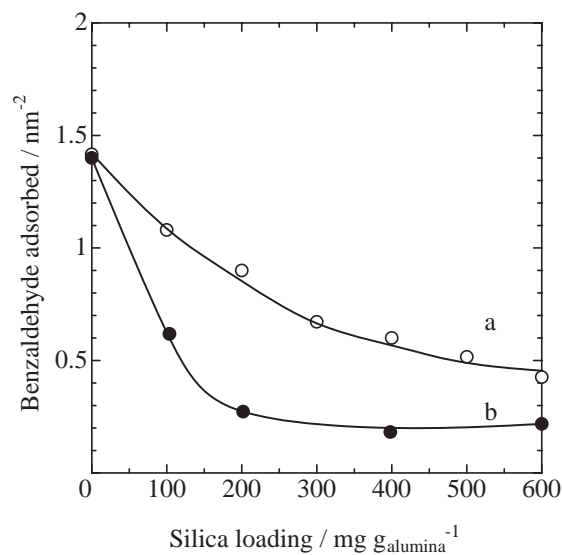


Fig. 6. Change in density of adsorption site of benzaldehyde on SiO₂-Al₂O₃. a, samples A; b, samples B.

benzaldehyde with silica loading. Benzaldehyde adsorbs on pure Al₂O₃ with a density of 1.4 nm⁻², while it does on the commercial silica gel at a small density of ca. 0.02 nm⁻².² Niwa et al. reported that the density of benzaldehyde adsorbed on alumina and silica were 1.80 and 0.14 nm⁻², respectively.¹⁴ In series A, the adsorption density gradually decreases with

increasing silica loading to ca. 0.4 nm^{-2} at $600 \text{ mg g}_{\text{alumina}}^{-1}$ (Fig. 6a). In contrast, the density of benzaldehyde adsorption sites steeply decreases in series B, and keeps a constant 0.2 nm^{-2} at silica loadings above $200 \text{ mg g}_{\text{alumina}}^{-1}$ (Fig. 6b).

Acidic and Catalytic Properties of Silica-Coated Alumina. Figure 7 shows the TPD profiles of NH_3 adsorbed on silica-coated alumina. The acid strength as a function of desorption temperature and the number of acid sites are estimated by the profile. Table 3 lists the number of acid sites, acid density, and ratio of Si/acid site. Silica deposition creates acidic sites on the alumina surface: the number of acid sites increases with silica loading reaching a maximum at $400 \text{ mg g}_{\text{alumina}}^{-1}$ in series B.

Figure 8 shows the temperature dependence of the catalytic activity of silica-coated alumina samples in the cracking of cumene. The conversion of cumene, which increases with

temperature, depends on the sample. The sample B-400 has the highest catalytic activity, superior to those of a commercial silica-alumina and A-400. The commercial silica-alumina, N631L, is reported to be an excellent catalyst for several acid-catalyzed reactions.⁶ The catalytic data in the temperature range between 400 and 500°C are also summarized in Table 2. In series A, A-500 shows the highest catalytic activity, which is comparable to that of the commercial silica-alumina. Figure 9 shows changes in the catalytic activity of both series for the cracking of cumene at 450°C with silica loading. Excess silica loading decreases the catalytic activity in both series (A-600 and B-600). At silica loading of $>200 \text{ mg g}_{\text{alumina}}^{-1}$, the series-B samples show higher catalytic activity than the A samples do.

Discussion

Silica Deposition on $\text{Al}(\text{OH})_3$. Various metal oxides coated with a thin silica layer were prepared by liquid-phase deposition methods using tetraethoxysilane (TEOS).^{1,2} The TEOS treatment is more effective for depositing silica on the precursor hydroxides than the hydrothermal treatment employing the dissolution-deposition of silica. The silica-coated metal oxides of MgO , Fe_2O_3 , NiO , Y_2O_3 , ZrO_2 , SnO_2 , and Dy_2O_3

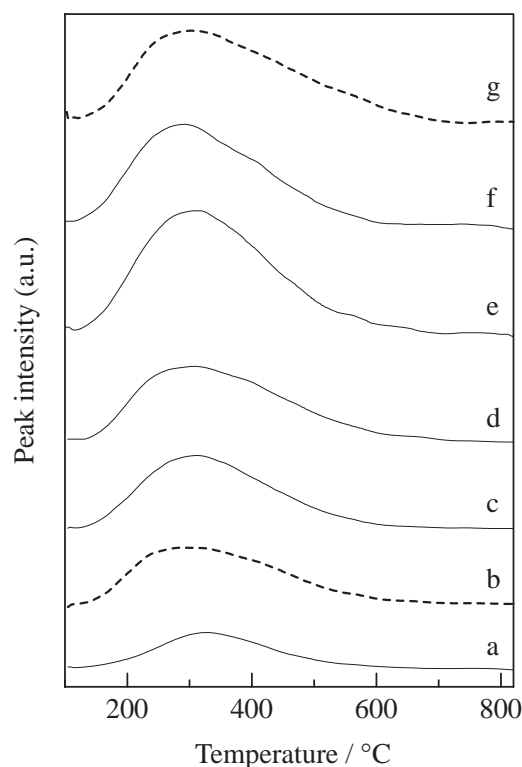


Fig. 7. TPD profiles of adsorbed NH_3 . a, Al_2O_3 ; b, sample A-400; c, B-100; d, B-200; e, B-400; f, B-600; g, commercial silica-alumina.

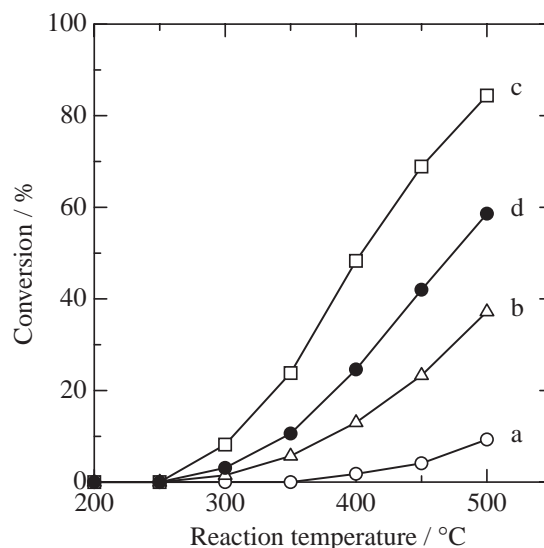


Fig. 8. Temperature dependence of catalytic activity of $\text{SiO}_2\text{-Al}_2\text{O}_3$. a, sample B-100; b, B-200; c, B-400; d, commercial silica-alumina.

Table 3. Acidic Property of SiO_2 -Coated Al_2O_3 ^{a)}

Catalyst ^{b)}	Number of acid sites		Ratio of Si/acid site	Density of adsorbed benzaldehyde/ nm^{-2}
	$/\mu\text{mol g}^{-1}$	$/\text{nm}^{-2}$		
Al_2O_3	155	0.31	—	1.4
A-400	282	0.49	23.7	0.6
B-100	323	0.63	5.1	0.6
B-200	382	0.78	8.7	0.3
B-400	558	1.08	11.9	0.2
B-600	457	0.90	21.9	0.2
N631L ^{c)}	445	0.66	—	—

a) Estimated by NH_3 desorbed in TPD measurement. b) Calcined at 500°C for 3 h. c) A commercial silica-alumina.

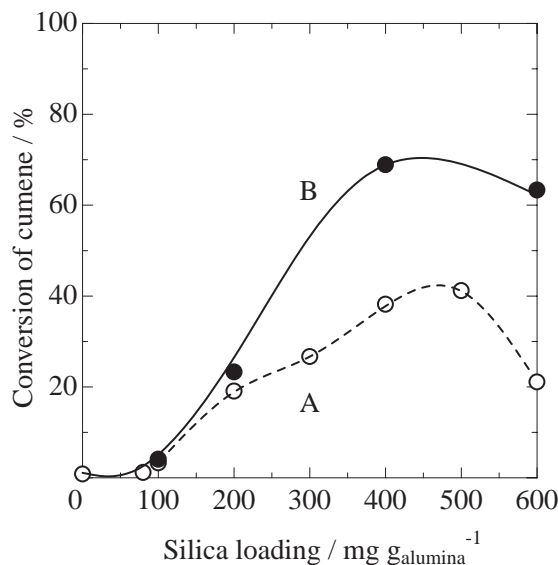


Fig. 9. Changes in catalytic activity with silica loading of SiO₂-Al₂O₃ at 450 °C. (A) series-A and (B) series-B samples.

have high specific surface areas $>200 \text{ m}^2 \text{ g}^{-1}$ after heating at 773 K.¹ The deposited silica prevents the agglomeration of core oxide particles during calcination: the high specific surface area of the precipitate is retained even after calcination.¹⁻⁴ However, aluminum hydroxide consists of large particles, with a SA of $30 \text{ m}^2 \text{ g}^{-1}$ (Table 1). This is the significant difference from the other metal oxides reported previously.

The results in Table 1 indicate that the transformation accompanies the decomposition of a large Al(OH)₃ particle into small pieces of γ -Al₂O₃ particles at 300 °C. The results are consistent with the pioneering work on the preparation of alumina.^{11,12} In the same way, it is reasonable that the core Al(OH)₃ with the silica layer decomposed into small alumina particles with and without a silica layer during calcination (series A). The size of the core Al(OH)₃ is much larger than the calcined body of alumina.

In the pre-calcined body of A₀-80, the average thickness of the silica layer on Al(OH)₃ with a SA of $42 \text{ m}^2 \text{ g}^{-1}$ (Table 1) is calculated to be 0.8 nm, which is ten times as large as that on alumina. This is regarded as a limitation of silica deposition on hydroxide surfaces without a catalyst for the hydrolysis of TEOS. In other metal oxides, it is reported that silica deposits on Pr₆O₁₁ and Nd₂O₃ with a thickness of 0.8 nm without using a hydrolysis catalyst.¹ The thickness of 0.8 nm indicates a maximum thickness of the silica layer from TEOS at 40 °C.

In the pre-calcined body of sample A-400, for example, the average thickness of the silica layer formed on Al(OH)₃ is estimated to be at least 3 nm. The precursor decomposes into small pieces of alumina with silica during calcination. The resulting materials consist of alumina with silica and pure alumina that comes from inside the core Al(OH)₃. Namely, the series-A materials are a mixture of silica-alumina and pure alumina particles. Thus, in A-400, the silica size in the silica-alumina particles is several nm.

We have identified the chemical shifts of ²⁹Si NMR resonance of silica deposited on alumina in the vapor phase.⁷ Judge-

ing from the ²⁹Si NMR result, the silica on A₀-80 with the average thickness of 0.08 nm (Table 2) has a thin layer spot rather than aggregates of silica. The ²⁹Si NMR results support the above speculation: the signal of A-400 is sharper than that of B-400, and this indicates the silica in A-400 is larger than that of B-400. If the deposited silica forms either a multiple layer or a particle aggregate, the Q₄ silicon, Si(OSi)₄, resonance is observed at ca. -110 ppm.⁷ In at least a trilayer of silica, Si located in the middle layer shows the resonance at -110 ppm. In a bilayer silica, Si located in the top layer shows the resonance from -90, Si(OSi)₂(OH)₂, to -100 ppm, Si(OSi)₃(OH). Sample A-100 has the resonance peak at -110 ppm, even at a small silica loading of $100 \text{ mg g}_{\text{alumina}}^{-1}$, which shows the silica species agglomerate. Ammonium nitrate, acting as a catalyst of TEOS hydrolysis in the preparation of series-A samples, agglomerates silica species in the liquid phase. This consideration is also supported by the TPD results of adsorbed benzaldehyde: more alumina surface is surely exposed on the surface in series A (Fig. 6). We can conclude that the series-A samples consist of a mixture of pure alumina and alumina with silica aggregate.

Thermal Stability of Silica-Coated Oxides. Coating oxides sometimes act as an obstacle for the sintering of the core materials during heating. In a silica-alumina prepared by depositing silica on alumina, it has been known that the alumina core particles exhibit a heat resistance to sintering even at 1493 K.¹⁸⁻²⁰ In the opposite case of silica-alumina prepared by depositing alumina on silica gel, the surface alumina also prevents the silica support from sintering during hydrothermal treatment at 373–423 K.²¹ Also, silica-coated metal oxides of MgO, Fe₂O₃, NiO, Y₂O₃, ZrO₂, SnO₂, and Dy₂O₃ maintain a high SA of $>200 \text{ m}^2 \text{ g}^{-1}$ even after heating at 500 °C.¹

Here, we should note that aggregation of pure alumina proceeds during the calcinations from 300 to 500 °C (Table 1). The pure alumina calcined at 500 °C has a SA of $300 \text{ m}^2 \text{ g}^{-1}$, which is intrinsic to alumina.¹² It is obvious that the particle size of the support is enlarged in both series of silica-alumina. The thermal stability seems to attribute to the high SA values, $350\text{--}400 \text{ m}^2 \text{ g}^{-1}$, of the present silica-coated alumina.

In the comparison of SA' based on the weight of core alumina between series A and B (Table 2), we notice an idea of thermal stability. It is obvious that series-B samples have the same type of thermal stability mentioned above: SA' of B-600 is consistent with the value of SA of alumina calcined at 300 °C. Namely, the size of alumina is maintained at 500 °C in the sample. In series-A, however, A-600 has a much higher SA' than $450 \text{ m}^2 \text{ g}^{-1}$. This indicates that deposited silica itself contributes the surface area. It is reasonable that silica aggregates themselves contribute a considerable portion of SA. In other words, the high SAs of series A are caused by the samples consisting of a mixture of silica-deposited alumina and pure alumina particles, as discussed in the previous section. Here, we should note that aggregation of core alumina proceeds during the calcination at 500 °C, even in the samples with a silica loading less than $200 \text{ mg g}_{\text{alumina}}^{-1}$ (A-200 and B-200).

Silica Deposition on γ -Al₂O₃. In sample B-100, the silica species deposited on alumina can be regarded as a monolayer because of the major peak at -80 ppm (Fig. 5), which is probably attributed to the Si(OAl)₂(OH)₂ structure.^{1,7,22,23} In B-200,

the deposited silica species can be regarded as a bilayer because of the major peaks at -90 and -100 ppm, which are attributed to the representative structures of $\text{Si}(\text{OSi})_2(\text{OH})_2$ and $\text{Si}(\text{OAl})_2(\text{OSi})_2$, respectively.⁷ The silica species deposited on B-400 can be regarded as a trilayer because of the major peaks at -90 , -100 , and -110 ppm, which are attributed to $\text{Si}(\text{OSi})_2(\text{OH})_2$, $\text{Si}(\text{OAl})_2(\text{OSi})_2$, and $\text{Si}(\text{OSi})_4$ structures, respectively.⁷

We have developed another silica–alumina by the vapor-phase deposition of silica on alumina with a SA of $203 \text{ m}^2 \text{ g}^{-1}$ from TEOS.⁶ The catalytic activity of silica–alumina varies with the silica loading depending on the reactions, such as dehydration, isomerization, and cracking: the most active species for the cracking of cumene has 19 wt % of silica, which corresponds to a silica density of 11.2 nm^{-2} .⁶ This has no significant difference from the present results (Table 2). In addition, a silica bilayer is observed on the alumina with silica content of 11.8 wt %, which is a silica density of 6.5 nm^{-2} .⁷

The present results of ^{29}Si NMR and TPD of BA indicate that the silica deposited on the alumina in series B consists of a thin layer rather than particle aggregates. In the present liquid-phase deposition, trilayer silica is the most active species, whereas further layers decrease the activity (A-600 and B-600). This is consistent with the previous reports.^{6,7} Thus, we can conclude that the silica trilayer produces the most active species in the cumene cracking.

In the acid-catalyzed cumene cracking, the series-B samples that consist of silica-coated oxide particles are superior to the series-A samples, which consist of a mixture of pure alumina and alumina with silica aggregate. The difference in the silica structure (Figs. 5 and 6) causes the difference in the acidity (Fig. 7) and the catalytic activity (Fig. 9). In the present liquid-phase process, the high SA of the support could be effective in dispersing silica as not to aggregate the core metal hydroxide under mild deposition conditions. This is the great advantage in depositing silica on support materials such as alumina.

Conclusion

SiO_2 -coated Al_2O_3 powders were prepared by depositing silica on the hydroxide and oxide of aluminum using tetraethoxysilane (TEOS) under different conditions at 40°C . On an $\text{Al}(\text{OH})_3$ precipitate with a large particle size and SA of $40 \text{ m}^2 \text{ g}^{-1}$, silica loading was saturated at only $80 \text{ mg g}_{\text{alumina}}^{-1}$ without using a catalyst for the hydrolysis of TEOS. The core $\text{Al}(\text{OH})_3$ was decomposed and crystallized to $\gamma\text{-Al}_2\text{O}_3$ during the calcination of the silica-coated $\text{Al}(\text{OH})_3$ at $>800^\circ\text{C}$, and the resulting $\text{SiO}_2\text{-Al}_2\text{O}_3$ have a SA of $>400 \text{ m}^2 \text{ g}^{-1}$.

When ammonium nitrate was used as a catalyst for the hydrolysis of TEOS, hydrolyzed TEOS could be deposited on $\text{Al}(\text{OH})_3$: The silica loading increased linearly with the increase in the amount of TEOS charged in the deposition vessel. The silica loaded on the $\text{Al}(\text{OH})_3$ aggregated during the deposition, and the core $\text{Al}(\text{OH})_3$ was decomposed and crystallized to a mixture of pure alumina and alumina with aggregated silica during calcination. Thus, the resulting $\text{SiO}_2\text{-Al}_2\text{O}_3$

also had a SA of $>350 \text{ m}^2 \text{ g}^{-1}$. However, the small SA of the support, starting $\text{Al}(\text{OH})_3$, has a disadvantage in generating active acid sites.

On $\gamma\text{-Al}_2\text{O}_3$ with the SA of $450 \text{ m}^2 \text{ g}^{-1}$, which was prepared by decomposing $\text{Al}(\text{OH})_3$ at 300°C , silica loading increased with increasing the amount of TEOS charged at 40°C without using ammonium nitrate. Silicate species uniformly covered the $\gamma\text{-Al}_2\text{O}_3$ surface with a thin layer. The SiO_2 -covered $\gamma\text{-Al}_2\text{O}_3$ showed higher catalytic activity in the cumene cracking than those of $\text{SiO}_2\text{-Al}_2\text{O}_3$ prepared from $\text{Al}(\text{OH})_3$ precipitate. We insist that the high SA of supports is necessary for generating more active acid sites in the silica deposition on alumina.

References

- 1 D. Shin, S. Sato, R. Takahashi, T. Sodesawa, *J. Ceram. Soc. Jpn.* **2002**, *110*, 1097.
- 2 S. Sato, R. Takahashi, T. Sodesawa, R. Tanaka, *Bull. Chem. Soc. Jpn.* **2003**, *76*, 217.
- 3 S. Sato, R. Takahashi, T. Sodesawa, S. Tanaka, K. Ogura, K. Ogura, *J. Catal.* **2000**, *196*, 190.
- 4 S. Sato, R. Takahashi, T. Sodesawa, N. Ichikuni, H. Amano, *Bull. Chem. Soc. Jpn.* **2002**, *75*, 2297.
- 5 S. Sato, M. Toita, Y. Q. Yu, T. Sodesawa, F. Nozaki, *Chem. Lett.* **1987**, 1535.
- 6 S. Sato, M. Toita, T. Sodesawa, F. Nozaki, *Appl. Catal.* **1990**, *62*, 73.
- 7 S. Sato, T. Sodesawa, F. Nozaki, H. Shoji, *J. Mol. Catal.* **1991**, *66*, 343.
- 8 T. Jin, T. Okuhara, J. M. White, *J. Chem. Soc., Chem. Commun.* **1987**, 1248.
- 9 M. Niwa, N. Katada, Y. Murakami, *J. Catal.* **1992**, *134*, 340.
- 10 G. A. Park, *Chem. Rev.* **1965**, *65*, 177.
- 11 C. Perego, P. Villa, *Catal. Today* **1997**, *34*, 281.
- 12 G. K. Chuah, S. Jaenicke, T. H. Xu, *Microporous Mesoporous Mater.* **2000**, *37*, 345.
- 13 M. Niwa, Y. Matsuoka, Y. Murakami, *J. Phys. Chem.* **1987**, *91*, 4519.
- 14 M. Niwa, K. Suzuki, M. Kishida, Y. Murakami, *Appl. Catal.* **1991**, *67*, 297.
- 15 S. Sato, M. Tokumitsu, T. Sodesawa, F. Nozaki, *Bull. Chem. Soc. Jpn.* **1991**, *64*, 1005.
- 16 S. Sato, K. Takematsu, T. Sodesawa, F. Nozaki, *Bull. Chem. Soc. Jpn.* **1992**, *65*, 1486.
- 17 M. Yabuki, R. Takahashi, S. Sato, T. Sodesawa, K. Ogura, *Phys. Chem. Chem. Phys.* **2002**, *4*, 4830.
- 18 B. E. Yoldas, *J. Mater. Sci.* **1976**, *11*, 465.
- 19 B. Beguin, E. Garbowski, E. Primet, *J. Catal.* **1991**, *127*, 595.
- 20 N. Katada, H. Ishiguro, K. Muto, M. Niwa, *Chem. Vap. Deposition* **1995**, *1*, 54.
- 21 S. Sato, R. Takahashi, T. Sodesawa, A. Miura, C. Kobayashi, K. Ogura, *Phys. Chem. Chem. Phys.* **2001**, *3*, 885.
- 22 T.-C. Sheng, S. Lang, B. A. Morrow, I. D. Gay, *J. Catal.* **1994**, *148*, 341.
- 23 N. Katada, M. Niwa, *Res. Chem. Intermed.* **1998**, *24*, 481.